

Automatic Adjustable Spraying Device for Site-Specific Agricultural Application

Ron Berenstein and Yael Edan, *Member, IEEE*

Abstract—This paper presents a device for accurate pesticide spraying capable of dealing with amorphous shapes and variable-sized targets. The device includes a single spray nozzle with an automatically adjustable spraying angle, color camera, and distance sensors, all mounted on a pan tilt unit. The site-specific spraying device aims to spray specific targets while reducing the use of pesticides. The spraying diameter is set as the minimum closing circle diameter according to the shape and size of the target. Two preliminary experiments were conducted in order to evaluate the spray nozzle flow rate in relation to the spray diameter and the spray diameter in relation to the nozzle's angular position. A main outdoor experiment was conducted to evaluate the complete spraying device using artificial targets of varying sizes. The results indicated that the spraying device is capable of reducing the amount of pesticides applied. An economic analysis estimates that up to 45% of pesticide reduction is possible when using the suggested spraying method. Actual savings depend on the spraying durations, target size, and distribution.

Note to Practitioners—This paper focuses on the development of a site-specific sprayer solution. The developed device aims to reduce pesticide application by spraying individual targets specifically by setting the diameter of the spraying according to the shape and size of the target. The core of the paper is a detailed description of a spraying device able to change its spraying diameter according to the detected target. A working procedure to calibrate and validate such a device is included. We believe that such a device can be used in modern agriculture and can be combined with a robotic sprayer navigating autonomously along crop fields. Such a device will contribute to reduced pesticide application.

Index Terms—Agricultural engineering, agricultural machinery, machine vision, precision agriculture, spraying.

Manuscript received June 18, 2016; revised October 19, 2016; accepted January 6, 2017. This paper was recommended for publication by Associate Editor A. Pashkevich and Editor Y. Sun upon evaluation of the reviewers' comments. This work was supported by the Helmsley Charitable Trust through the Agricultural, Biological and Cognitive Robotics Initiative and by the Rabbi W. Gunther Plaut Chair in Manufacturing Engineering, both at Ben-Gurion University of the Negev.

The authors are with the Department of Industrial Engineering and Management, Ben-Gurion University of the Negev, Beer-Sheva 8410501, Israel (e-mail: berensti@bgu.ac.il; yael@bgu.ac).

This paper has supplementary downloadable multimedia material available at <http://ieeexplore.ieee.org> provided by the authors. The Supplementary Material contains two videos. Main experiment video: The experiment conducted to evaluate the ASD performance under real-world conditions. The video shows how the robotic sprayer is advancing in a step mode along a red line strip fix to the ground. During each step, the ASD find the targets in the frame, adjust the ASD spraying diameter, and perform single spray. Target diameter evaluation: This video presents the process of evaluating the ASD spray diameter. The ASD diameter is evaluated by applying red spray and crossing the spray trajectory with a white paper sheet. The ASD spray diameter is later manually measured using a captured video similar to this. This material is 42.7 MB (13.9 MB and 28.8 MB) in size.

Color versions of one or more of the figures in this paper are available online at <http://ieeexplore.ieee.org>.

Digital Object Identifier 10.1109/TASE.2017.2656143



Fig. 1. Pesticide spraying methods. (a) Backpack sprayer: the human carries the pesticide and sprays manually. (b) Tractor sprayer: the human drives a tractor with spraying equipment.

I. INTRODUCTION

THE use of pesticides is an integral part of worldwide agriculture. Between 30% and 35% of crop losses can be prevented when harmful insects and diseases are eliminated by use of pesticides [1]. Although pesticides are necessary in modern agriculture, they are poisonous and dangerous for humans [2], [3] and for the environment [4], [5]. Current methods for pesticide application include a human operator traveling along the crop rows and selectively spraying the targets manually using a backpack sprayer [Fig. 1(a)], and mechanized nonselective spraying in which a human drives a tractor with a sprayer connected to a trailer behind the tractor that sprays the crops continuously [Fig. 1(b)]. Despite the use of pesticide protection equipment (personal head mask and central filtration system for the manual and mechanized spraying methods, respectively) the human is still exposed to hazardous pesticides that can cause negative health issues [6]. Besides health concerns, mechanized and manual spraying methods have other drawbacks. The mechanized spraying is not target specific and is designed to spray a crop strip with preadjusted height (e.g., for spraying just the grape clusters the farmer will preset the spray nozzles to spray a strip 0.5 m wide with no consideration of the fruit location). Furthermore, manual spraying is tedious work, slow, and limited due to the lack of workers in agriculture.

The use of spraying nozzles in modern industry is widespread for different applications such as cleaning [7], coating [8], fire suppression [9], and painting [10]. Manufacturers offer a wide range of nozzles with manually adjustable spraying angles and even automatic spraying systems that can control the flow rate (e.g., Spraying Systems co, PulsaJet, and AutoJet).

Due to the nature of the products and applications in the industrial domain, the nozzle spraying angle is preset manually according to the designated target, which is well defined. In the agricultural domain, the targets have inherent high variability



Fig. 2. Grape clusters captured from a commercial vineyard. (a) Grape clusters image. (b) Binary image of the same scene.

in size (e.g., watermelon and lettuce) and shape (e.g., grape clusters, cherry tomatoes, eggplant, kiwi, and strawberry) [11] that requires adjusting the spraying coverage to the specific target. This paper is focused on finding a spraying solution for these amorphous variable-shape and size objects aiming to spray individual targets specifically by setting the diameter of the spraying according to the shape and size of the target.

This paper is part of an ongoing research aimed to replace the traditional spraying methods with an agricultural robotic sprayer [12]. The robot navigates autonomously along the vineyard rows, and performs specific spraying toward detected targets [13]–[17]. For site-specific spraying the target must first be detected and then sprayed. This research focuses on the spraying process so as to completely cover the target while minimizing the amount of material sprayed. Ongoing research focused on the target detection (both autonomously [17] and with remote human supervision [14]–[16]) and on the development of a fully operational agricultural spraying robot [18].

The targets in this case study are grape clusters in commercial vineyards. The grape cluster's shape is amorphous with varying sizes and orientations. Fig. 2 shows the high variances of the grape clusters. The orientation, size, and shape are individual to each object in the scene.

Extensive research has been performed over the past two decades on spraying robots, mainly for the automotive industry [19], with a focus on path planning of the robotic arm and achieving uniform paint thickness layers [20]–[25].

Several agricultural spraying robots have been developed for weed control and plant protection applications [26]–[39] aiming to reduce the use of pesticides while preventing crop losses due to pests [40].

The goal of this paper was to develop an accurate, target-specific, spraying device that can replace the human operator. The novel spraying system aims to spray targets accurately and specifically without human intervention. The diameter of the sprayer is set according to the shape and size of the target similar to the recently proposed patent [41] that suggests a changeable nozzle aperture. However, in this paper, the proposed approach was designed, built, and implemented in real-world conditions and included experimental procedures and experiments for evaluation and validation of the spraying device for agricultural amorphous shapes and variable-sized targets.

Preliminary work was performed in order to analytically evaluate three optional methods for specific target spraying, focusing on the spraying technique to ensure full coverage of the detected target with minimum spray [13].

The evaluated spraying methods were as follows [13].

- 1) *Fixed Nozzle Spacing*: In this method, we assume that a set of nozzles are organized vertically on a spraying column with predetermined spacing. The nozzle position and the spray diameter are set prior to the spraying process regardless of the target's shape and size. While the sprayer vehicle travels along the crop row, the nozzles spray synchronously (using an electric valve) in order to cover the target.
- 2) *Optimal Spray Coverage*: In this method, we assume that the spraying is performed using a single spraying nozzle attached to a pan tilt unit (PTU) and is capable of directing the nozzle. The spray diameter of the nozzle is set prior to the spraying process. Since the spray diameter is fixed, each target will require several sprays for full coverage.
- 3) *One Target–One Shoot (OTOS)*: In this method, we assume that a spraying nozzle is attached to a PTU and can change the spraying diameter automatically. Using this method each target is sprayed once with a diameter that covers the entire target.

The analytical evaluation of these methods on 129 images captured from a commercial vineyard showed that the best method for spraying these targets is the OTOS spraying method [13]. Preliminary economic analysis indicated that the OTOS spraying method is advantageous for the farmer as long as the cost of pesticide waste is lower than $\$6/\text{m}^2$ [13].

The main contribution of this paper is the design, implementation, and experimental framework of a novel device that sprays targets accurately and specifically without the presence of a human operator. Economic analysis of the savings is provided.

II. ADJUSTABLE SPRAYING DEVICE

An adjustable spraying device (ASD) was designed and built as an experimental tool in order to implement the OTOS spraying method [13]. The device is mounted on a mobile robotic sprayer and supplies pressurized pesticide. The operational concept of the ASD is as follows:

- 1) direct the nozzle to face the crop (perpendicular to the crop);
- 2) capture an image using the ASD camera;
- 3) find the target's positions and diameters;
- 4) for each target perform the following routine:
 - a) direct the ASD toward the target center;
 - b) adjust the nozzle diameter to equal the closing circle diameter of the target; and
 - c) open the sprayer electric valve for a specific pre-defined duration.

The ASD is presented in Fig. 3(a)–(c). The ASD base is constructed from three aluminum parts, two pressure plates that mount the spraying nozzle and the two line beam lasers, and a shoulder. The shoulder is connected to the pressure plate with four screws and can be height adjusted.

The ASD was based on a commercial spraying nozzle (AYHSS 16) using the recommended spraying pressure of 20 bar. The spraying nozzle is constructed from two parts, the nozzle base and the nozzle cup. The nozzle base is mounted on the pressure plates. The pressurized pesticide hose is connected

to the nozzle base and the flow is controlled using an electric valve (ON/OFF). The spraying diameter can be controlled by rotating the nozzle cap over the nozzle base. This nozzle was chosen as it is in common use among farmers who adjust the spraying diameter prior to the spraying task.

A stepper motor, mounted on the shoulder, is used to control the spraying diameter. The stepper motor is connected to the nozzle cap using two tangent gears, one connected to the stepper motor [Fig. 3(a), black gear and 28 tooth] and the other connected to the spraying nozzle cap [Fig. 3(a), white gear and 42 tooth]. The stepper motor is controlled using a digital stepper motor driver (LEADSHINE DM556). Rotational feedback of the stepper motor is acquired using a rotational potentiometer (10 rounds, 1 K Ω) connected to the stepper motor gear. An Arduino (uno) board closes the stepper motor position loop using feedback from the potentiometer and the desired circular position.

Other peripheral sensors are mounted on the ASD; a laser distance sensor (SICK DX35) for measuring the distance between the device and the target, a color camera (Microsoft studio cam) for capturing images from the field for automatic target detection, and two-line beam marking lasers (532 nm, 50 mW, 60°) positioned horizontally and vertically for marking a cross (+) over the target. The entire device is mounted on a PTU (FLIR D46-17) able to rotate horizontally $\pm 180^\circ$ and vertically $+31^\circ$ up to -80° .

A PC computer is connected to an Arduino board, laser distance sensor, color camera, PTU, and the electric valve controlling the pesticide flow. The main software for managing the ASD was based on Microsoft Visual Studio (c#). The software collects data from the ASD sensors and controls the ASD orientation by adjusting the PTU, the ASD nozzle by rotating the stepper motor, and the electric valve opening/closure, according to the collected data.

III. SPRAYING DEVICE PRELIMINARY EXPERIMENTS

Two preliminary experiments were conducted in order to evaluate the pesticide flow rate and the spray deposition with different nozzle apertures.

A. Flow Rate Evaluation

A flow rate experiment was performed to evaluate the pesticide flow rate for varying spraying nozzle apertures. The experimental setup included setting up a spraying pressure of 20 bar (the recommended pressure for this type of spraying nozzle). The spraying duration was controlled by a computer using the electric valve.

Twenty-one nozzle apertures that cover the full rotation scale of the nozzle were measured. For each aperture, three sprays were measured with a 4 s delay between the measurements (the delay was derived empirically to allow the remaining drops to leave the nozzle orifice). The duration of each spray was 1 s. The sprayed material was tap water.

The flow rate evaluation results (Fig. 4) show the relation between the flow rate and the corresponding angular position of the nozzle cup.

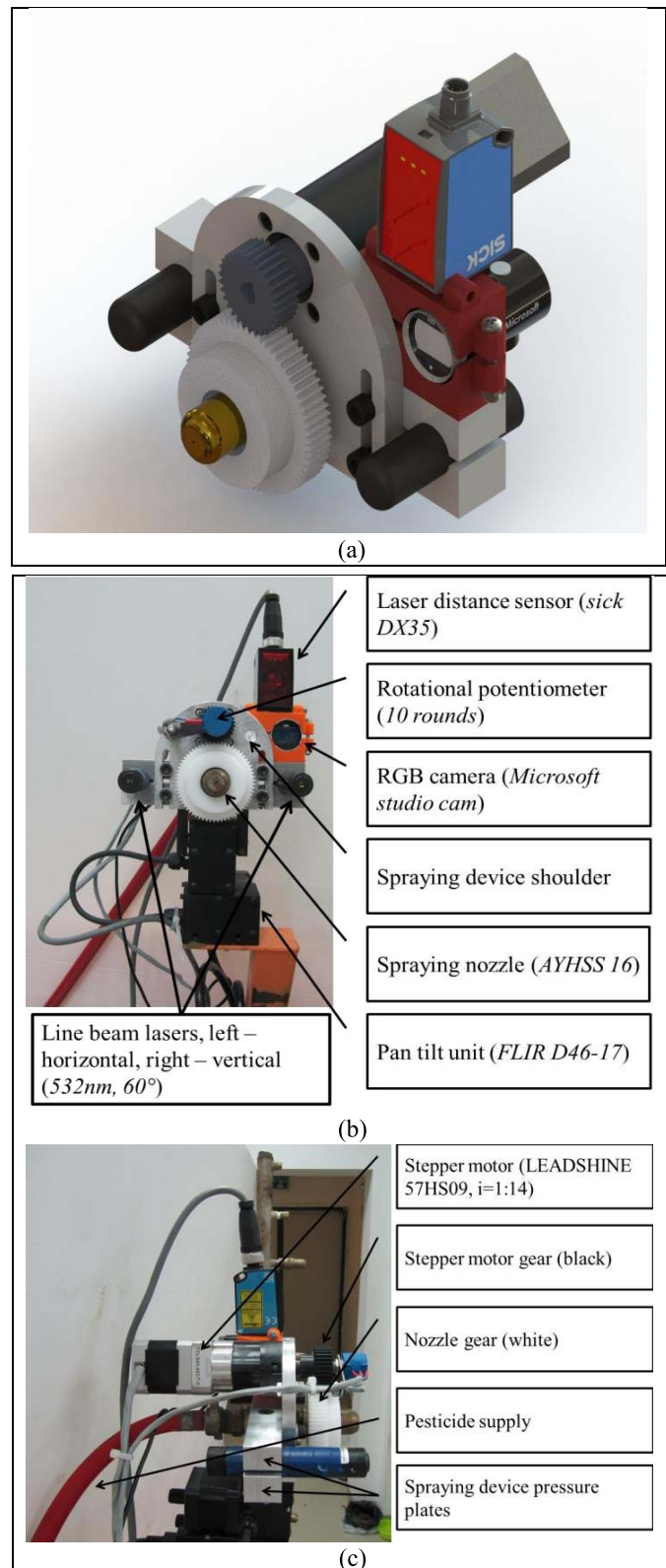


Fig. 3. Spraying device. (a) Isometric view-CAD. (b) Front view. (c) Side view.

B. Spray Diameter Evaluation

The spray diameter (spray cone) for varying nozzle apertures was evaluated to enable adjustment of the nozzle aperture to correspond to the target size.

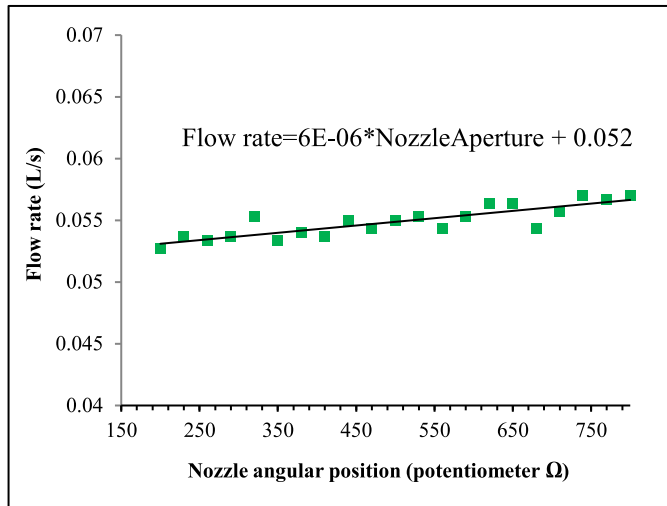


Fig. 4. Flow rate evaluation results. Angular position of the nozzle cup was measured using the rotational potentiometer attached to the stepper motor gear.

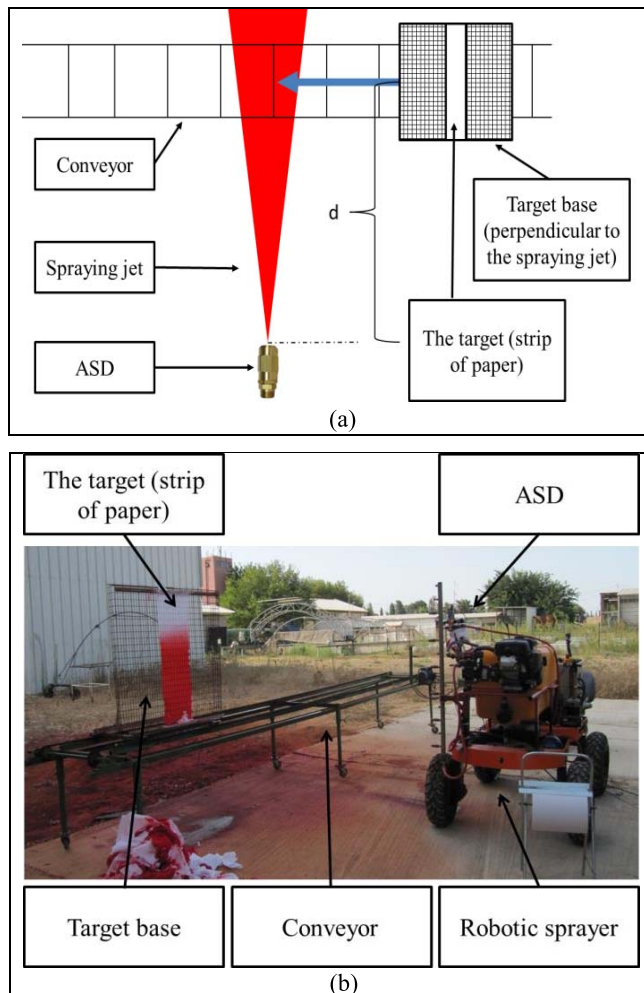


Fig. 5. Configuration of an experiment for spray diameter evaluation. (a) Experimental scheme. (b) Field view of the experiment.

The experimental setup [Fig. 5(a) and (b)] included the ASD facing the target base with a target attached. The target base was constructed from steel net and was mounted vertically on a manually controlled conveyor in front of the ASD [Fig. 5(b)]. The target used was a white paper sheet, 0.5 m wide, which

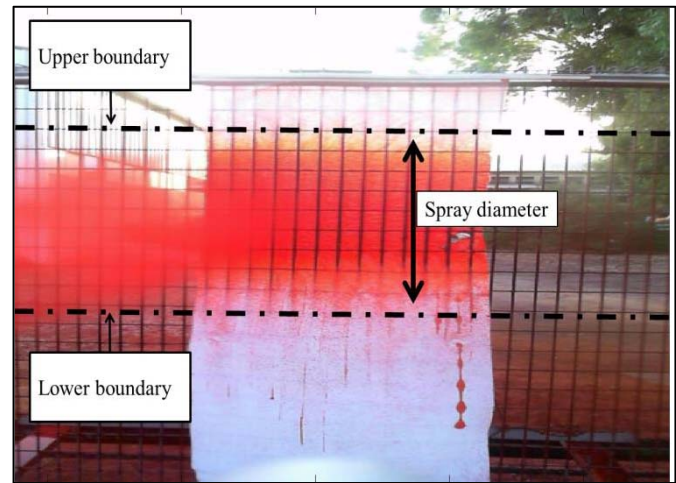


Fig. 6. Example of a single frame extracted from captured spraying movie. Using the captured frame, the boundaries (upper and lower) and the spray diameter of the sprayed target were extracted.

was stretched from top to bottom and fixed to the target base [Fig. 5(b) shows the target fixed to the target base after spraying]. In order to view the spray deposition and postanalyze the position of the spray, a red water-soluble food dye (Florma red 696) was used as pesticide replacement.

Each spray repetition included the following steps: 1) attaching a new target to the target base; 2) setting the nozzle aperture to the desired value; 3) opening the spray flow; 4) starting the conveyor movement toward the spray jet; and 5) after the entire target base has crossed the spraying jet, the spray flow is closed and the conveyor stops. To focus on the ASD operation only it was important to ensure that the ASD was operated in static conditions. Hence, it was operated when the robot was not moving.

Image acquisition software was designed to capture a movie along the spray process. After each spray repetition, the captured movie was saved for postanalysis. Each movie was manually scanned by a human expert to extract a single frame containing the target in midframe. The extracted frame was analyzed manually for the spray boundaries (Fig. 6). As the spray has a cone-base shape, the spray diameter was evaluated by measuring the distance (in pixel units) between the upper and lower spray boundaries.

Experiments were performed at three distances between the ASD and the target (0.5, 1, and 1.5 m). For each distance the nozzle angular positions were set between 175 and 210 with increments of 5 (units in potentiometer Ω). Three measurements were conducted for each distance-aperture combination.

All experiments were performed at dawn ensuring no-wind conditions (this was confirmed by measuring the wind speed using Skywatch Xplorer 1).

The experimental results shown in Fig. 7 reveal the relation between the nozzle aperture and the spray diameter for three measured distances. The measured spray diameter increases as the distance increases. In theory, the three curves are supposed to unite since both the camera field of view and the spraying cone have a linear trajectory. The spray dispersion is probably caused by the spray jet turbulence and air drag that affects the spray dispersion.

TABLE I
SUMMARY OF EXPERIMENTAL RESULTS

Distance	Trend line (power)	R ²
500	NA=600.22·SD ^{-0.210}	0.911
1000	NA=490.97·SD ^{-0.184}	0.782
1500	NA=467.12·SD ^{-0.177}	0.761

NA nozzle aperture; SD spray diameter

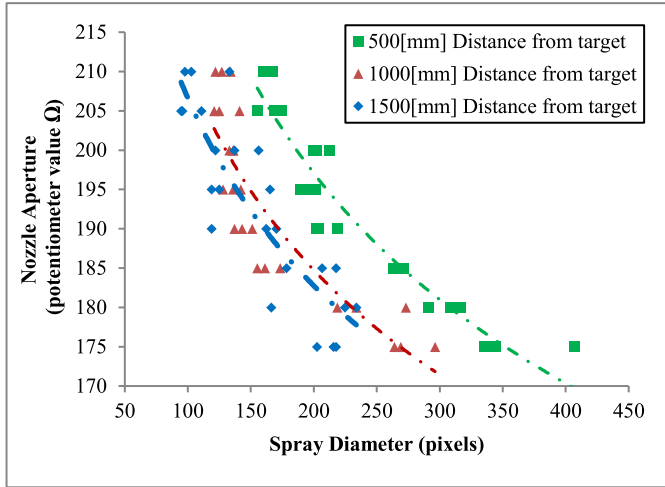


Fig. 7. Experimental results of the spray diameter for three measured distances.

The spray diameter increases with the increase in distance between the nozzle and the target (Fig. 7). This is because in the experiment the spray diameter is measured using the digital camera, which is located at the same distance as the spraying nozzle [Fig. 3(b), the spraying nozzle and the camera are located together], and is expressed using pixels units. Hence, in reality, the measured spray diameter does not increase with the increase in the distance, but remains approximately constant due to the digital camera perspective.

Table I presents the curve fitting parameters for Fig. 7, where NA is the nozzle aperture and SD is the spray diameter.

Using the resulting curves for the different distances, the nozzle aperture can be calculated after extracting the target diameter. The spraying distance in most commercial vineyards is between 500 and 1500 mm. In order to correlate between the spraying distance and the nozzle aperture, an interpolation of the distance and the nozzle aperture can be applied.

IV. EVALUATING THE ASD PERFORMANCE

An experiment was conducted in order to evaluate the performance of the ASD while implementing the results of the previous experiment (Table I). To focus the evaluation on the spraying device only, the robotic sprayer is designed to perform the spraying task in step mode (Fig. 8): the robot travels a single step along the vineyard row, stops, captures image from the field, sprays the targets, and moves another step forward. Hence, the spraying operation is performed while the robot is static (the operation of the ASD occurs only when the robotic platform is not moving).

One of the secondary goals of this experiment was to provide insights into the overall work procedure of the complete

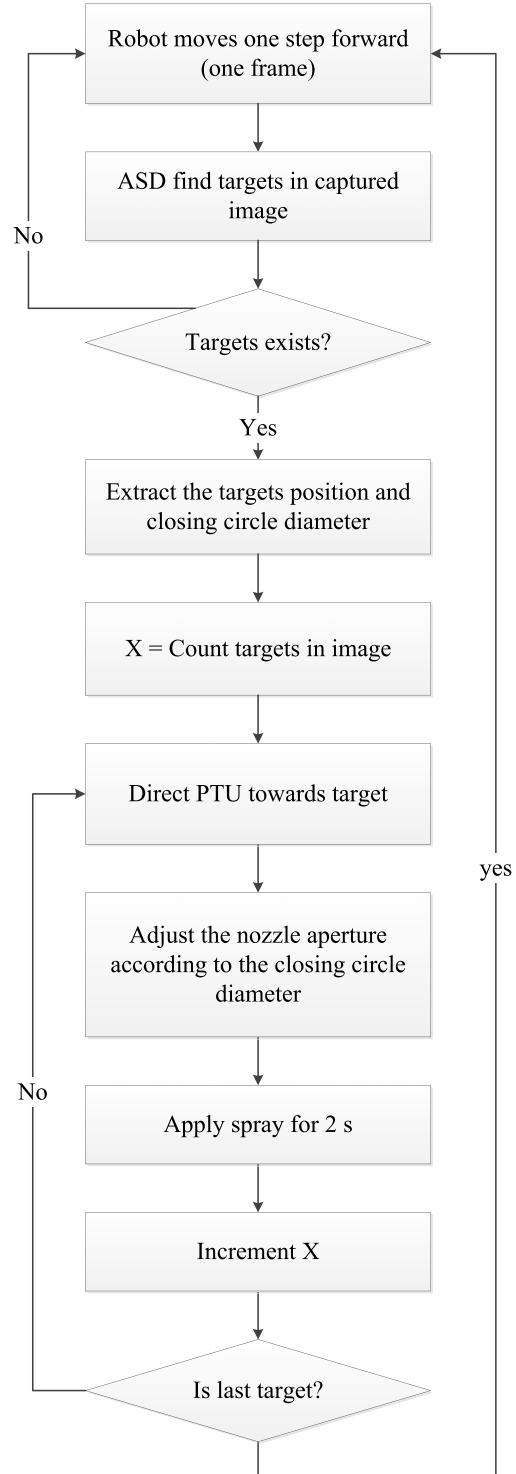


Fig. 8. Robotic sprayer work procedure. The following experiment procedure was based on this figure procedure, including the steps of directing the PTU toward the target core, adjusting the spraying nozzle, and the actual spraying.

spraying system, which will include the robot equipped with an ASD.

A. Experimental Setup

During the experiment the ASD was attached to the robotic sprayer, which as aforementioned, was operated in step mode while advancing along the vineyard row (Fig. 8). During this

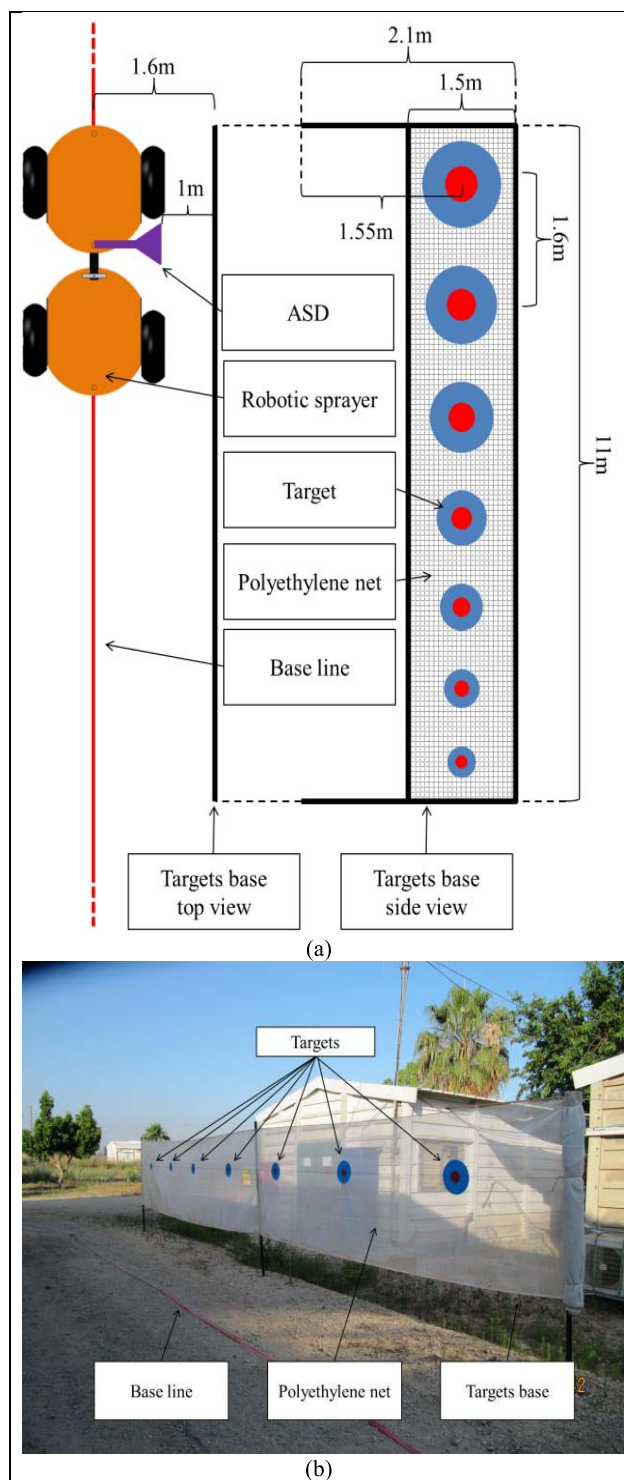


Fig. 9. Experiment configuration. (a) Experimental scheme. (b) Field view of the experiment.

experiment, the robotic sprayer was programmed to track a straight baseline placed at a 1.6 m distance from the target base (red plastic strip 50 mm width) [Fig. 9(a)]. The robot was programmed to travel 1.6 m at each step. The ASD is mounted perpendicular to the robot's travel direction and faces the target's base [Fig. 9(a)]. The target's base is a polyethylene net (50 mesh), 11 m long, stretched between two anchoring targets that were used in the experiments and it is not the core of this paper. Needless to say that in order to use the

attached to the target's base and the center of the target is positioned 1.55 m high. In order to ensure a single target per image, the targets were positioned at intervals of 1.6 m, similar to the robot's travel distance.

The targets are blue polyethylene round circles with varying diameters (300, 250, 230, 210, 190, 170, and 150 mm). To simplify the detection and classification of the targets, a red circle was attached to the center of the main target. The diameter of the red circle was one-third of the blue circle diameter.

Artificial targets were used to enable accurate target detection. The targets consisted of a round blue, polyethylene with different diameters (150, 170, 190, 210, 230, 250, and 300 mm). A round red, polyethylene target was mounted at the center of the blue target. The diameter of the red target was a third of the blue corresponding target [Figs. 9(b)–11].

The target detection algorithm was based on color thresholding and was implemented using MATLAB software equipped with the image processing toolbox as follows:

- 1) capture input RGB image (800×600) [Fig. 10(a)];
- 2) create three ratio images, green/red, blue/red, blue/green [Fig. 10(b)–(d), respectively];
- 3) threshold the ratio images. The threshold value was set as the average image pixel value multiplied by 1.5 [Fig. 10(e)–(g)];
- 4) merge (logical AND) the resulting binary images [Fig. 10(h)];
- 5) fill holes in the image using morphological operations (using MATLAB command *imfill*) and apply the removal of small clusters (<500) that are considered as noise (using MATLAB command *bwareaopen*) (Fig. 10(i));

The next steps were developed to distinguish between true and false targets and were applied to each of the detected targets;

- 6) isolate the bounding box of the target [Fig. 10(j)];
- 7) convert the RGB image into HSV representation and isolate the hue and saturation channels;
- 8) apply thresholds on the hue channel (with a scale of $0 \sim 1$, hue >0.9 , and hue <0.1) to extract the red area [Fig. 10(k)];
- 9) count the number of red pixels and compare with the number of blue pixels. In theory, the outcome ratio value should be 9; however, since the images are acquired in real-world conditions, the ratio allowed is according to the following conditional statement: $7 < (\text{blue} + \text{red}/\text{red}) < 11$. If the conditional statement is true then the detected target is defined as a true target, else, it is noted as a false detected target [Fig. 10(l)].

Following the detection process the program extracts the coordinates of the detected target's center and the minimum closing circle diameter in pixel units. These measures are used to control the sprayer (i.e., direct the PTU toward the target center and adjust the spraying diameter according to the closing circle diameter).

The target detection algorithm, with all of its steps and unique values, was developed specifically for the artificial targets and it is not the core of this paper. Needless to say that in order to use the

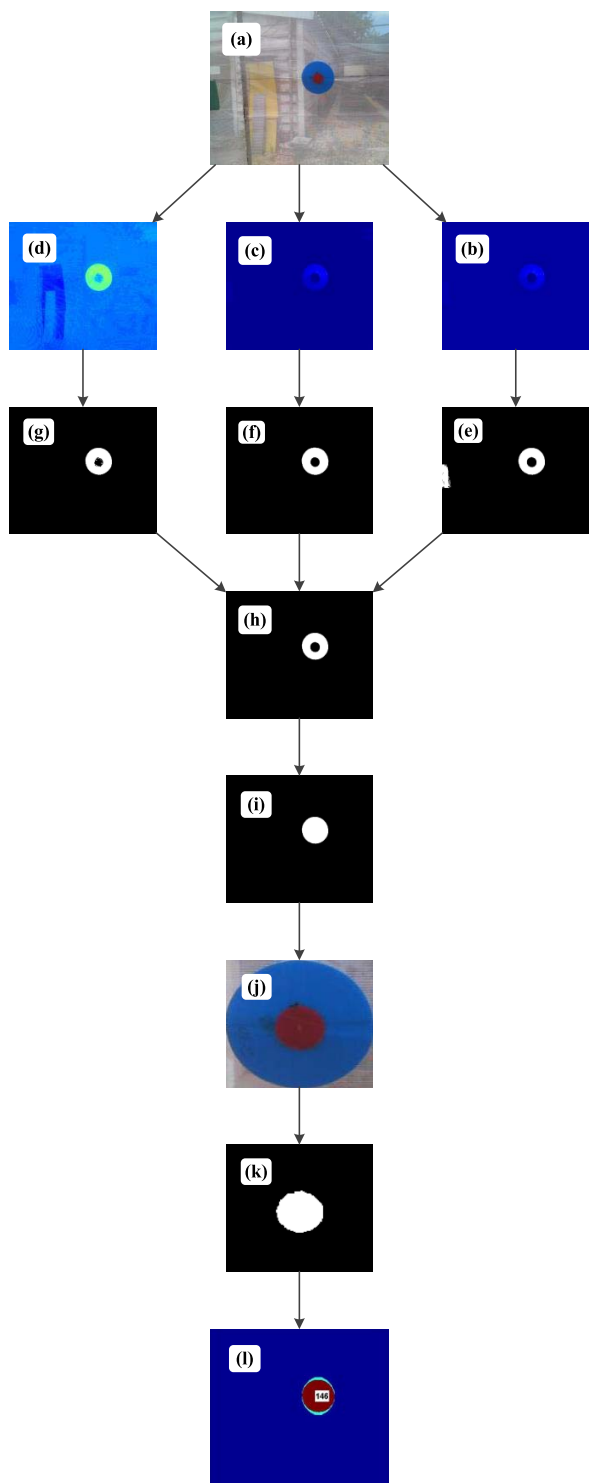


Fig. 10. Target detection procedure. Algorithm output image (l) shows the detected target (red) and the surrounding circle (light blue). Number in the circle represents the diameter of the surrounding circle needed to cover the entire target.

suggested ASD, a specific target detection algorithm must be developed for the specific crop (see [17]).

Similar to the previous experiment, a red water-soluble food dye (Florma red 696) was used as pesticide replacement to ease detection of the spray deposition.

The sprayed area was evaluated both manually by measuring the sprayed area's diameter immediately after each spray, and



Fig. 11. Image captured immediately after spraying.

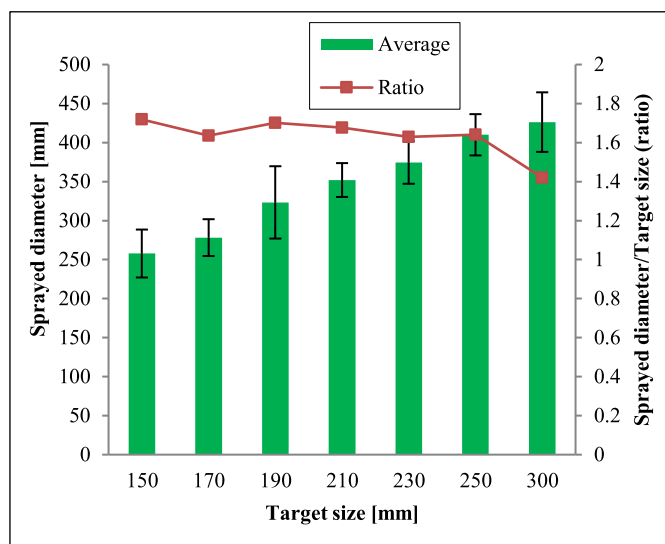


Fig. 12. Experimental results. Each column represents the average sprayed diameters of 12 sprays (robot repetitions). Results are standard deviations shown in each column. Red line (secondary axis on the right) measures the ratio between the sprayed diameter and the target size.

by image processing of images captured immediately after each spray (Fig. 11).

B. Experimental Design

The experiment included 12 repetitions of the robot traveling along the baseline and spraying the seven targets attached to the target base. Each target was sprayed for 2 s. All the experiments were conducted early morning. The measured wind speed was zero in all the experiments (measured using Skywatch Xplorer 1).

C. Experimental Results

The results described here use the ASD in automatic mode: the ASD automatically directs the PTU toward the target center and adjusts the spray diameter according to the closing circle diameter of the detected artificial target.

A visual inspection revealed that each target was fully covered by the spray (as noted in Section II and in Fig. 11). The experimental results are summarized in Fig. 12. The spray

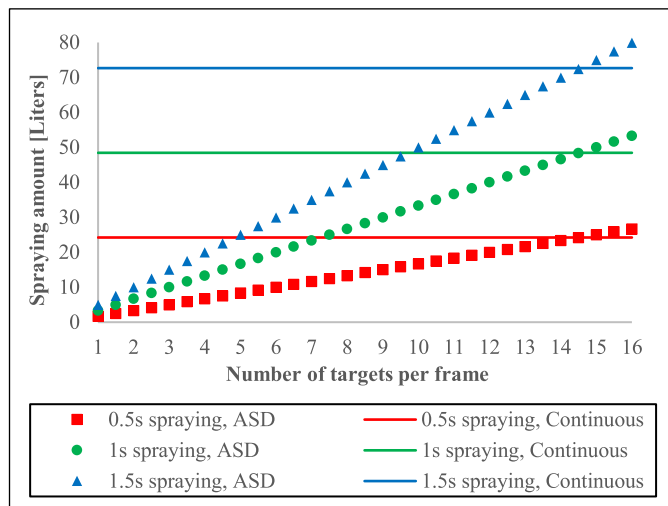


Fig. 13. Pesticide usage estimation. Graph shows the estimated amount of pesticide use while using both the ASD and the traditional spraying method for three spraying durations.

flows under gravitational force (Fig. 11) increasing the spray spot size, which complicates the spray diameter analysis and was thus eliminated from the spray diameter evaluation.

The results of the automatically adjustable spray diameter show a constant increase in the sprayed diameter with increase in target size; however, the ratio between the sprayed diameter and the target size decreases. This ratio can be addressed as the false detection ratio, and according to Fig. 12 this ratio decreases with increase in the target size. The 150 mm diameter target was sprayed with a coverage diameter of ~ 250 mm, whereas a 300 mm diameter target was sprayed with a coverage of ~ 425 mm. Hence, the amount of material saved increases as the size of the target increases.

D. Spraying Reduction Estimation

Potential pesticide reduction was calculated by comparing the ASD spraying with the traditional continuous spraying method [Fig. 1(b)]. The analysis was conducted for the ASD spraying method performed using a robotic sprayer working in step mode as described above, and the traditional spraying method applied using a robotic sprayer that travels along the row at a constant speed with three nozzles constantly open.

Evaluations were conducted for three spraying durations (the duration the nozzle is open to spray) and several number of targets per frame, as shown in Figs. 13 and 14. The estimation was calculated for spraying on one side of a single 100 m row of a commercial vineyard.

The results (Figs. 13 and 14) reveal that approximately 14 targets per frame is the equilibrium point between the two spraying methods. For less than 14 targets per frame it is recommended to use the ASD method and *vice versa*. The reduction in spraying material decreases as the number of target spraying times increase as expected.

Reduction of 45% (39.41 and 72.66 l for the ASD and traditional spraying, respectively) of spray material is achieved for the experimental conditions of 7.89 targets per frame

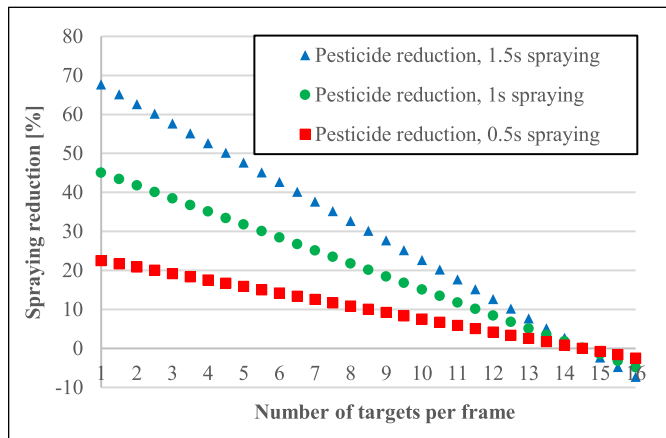


Fig. 14. Pesticide reduction estimation. Graph shows the estimated amount of pesticide that can be reduced while using the ASD spraying method instead of the traditional one. It is recommended to use the ASD method for all positive values. Traditional spraying method is preferable for negative values.

(corresponds to [13] and data evaluated from a commercial vineyard located in Israel during the growing season of 2009) and a 0.33 m/s robot traveling speed (corresponds to the recommended forward speed when using nozzles with a spray diameter of 0.33 m).

V. DISCUSSION AND CONCLUSION

The suggested device and spraying method enable to perform the spraying task efficiently and economically. The main contribution of this paper is in developing and evaluating a novel spraying device that ensures full coverage of the detected target with minimum spray. Pesticide application is reduced by spraying each target individually. This is achieved by directing the spraying device toward the center of the target using a PTU and setting the diameter of the spraying according to the shape and size of the target (according to the closing circle diameter of the target). The suggested ASD can be incorporated for different agricultural crops and for a variety of commercial applications. However, for each crop/application, specific target detection algorithms must be developed.

The overall spraying duration for a single target was 11 s. This duration included general software commands, communication between main software and peripherals (MATLAB, Arduino), machine vision, PTU repositioning, spraying nozzle aperture adjustment, spraying, and capture of image postspraying. It also included some software pauses located at critical points in the software. These pauses were used to control the experiment and to verify that the ASD was functioning as designed. The accumulated time of the pauses was 8 s and the spray time was 2 s. By eliminating the software pauses, the spraying time for a single target can be reduced to 3 s including the 2 s spraying time. Further time reduction can be achieved by optimizing the machine vision algorithms and the overall ASD control software. The spraying can also be achieved while the robot continuously advances along the row. However, to achieve this, the future work should address the implementation of the ASD operation while the robot platform advances along the row (i.e., with no stops).

While applying the traditional spraying method, the robot speed can be doubled by adding a parallel spraying nozzle to each existing one. However, the agronomic effect of this must be evaluated in the future research in actual growing conditions before application. Furthermore, the reduction of pesticides application achieved must be analyzed in real-world conditions for different speeds along with agronomic tests.

As the results revealed reduction in spraying material decreases as the number of targets' spraying times increase as expected, and there is an equilibrium point between the two spraying methods. For less than 14 targets per frame, it is recommended to use the ASD method and *vice versa*. The results also indicated that the amount of material saved increases as the size of the target increases, implying advent of the technology as the crop grows along the season.

The ASD can be operated independently (for spraying moving objects using a conveyor) or equipped on a mobile robotic platform. For full robot operation crop-specific target detection algorithms must be developed (see [17]). Navigation algorithms with corresponding sensors must also be implemented (see [42]). Actual pesticides savings depends on the performance of the detection and navigation algorithms, hence these must be validated in the future experiments to ensure economic feasibility. The future work should also deal with specific crops, pests, and pesticides including evaluation of the spraying characteristics and their agronomic effect (e.g., droplet size, droplet spread, spray surrounding coverage, and different spraying material) and include both real-time and economic performance evaluation.

ACKNOWLEDGMENT

The authors would like to thank Prof. A. Gamliel for his excellent guidance on the evaluation of the experiments.

REFERENCES

- [1] S. I. Cho and N. H. Ki, "Autonomous speed sprayer guidance using machine vision and fuzzy logic," *Trans. Amer. Soc. Agricult. Eng.*, vol. 42, no. 4, pp. 1137–1144, 1999.
- [2] S. Dasgupta, C. Meisner, D. Wheeler, K. Xuyen, and N. T. Lam, "Pesticide poisoning of farm workers—Implications of blood test results from Vietnam," *Int. J. Hygiene Environ. Health*, vol. 210, no. 2, pp. 121–132, 2007.
- [3] W. J. Rogan and A. Chen, "Health risks and benefits of bis(4-chlorophenyl)-1,1,1-trichloroethane (DDT)," *Lancet*, vol. 366, no. 9787, pp. 763–773, 2005.
- [4] D. Pimentel and H. Lehman, *The Pesticide Question: Environment, Economics, and Ethics*. London, U.K.: Chapman & Hall, 1993.
- [5] J. Reus *et al.*, "Comparison and evaluation of eight pesticide environmental risk indicators developed in Europe and recommendations for future use," *Agricult. Ecosyst. Environ.*, vol. 90, no. 2, pp. 177–187, 2002.
- [6] S. H. Swan *et al.*, "Semen quality in relation to biomarkers of pesticide exposure," *Environ. Health Perspect.*, vol. 111, no. 12, pp. 1478–1484, 2003.
- [7] J. Canny, "A computational approach to edge detection," *IEEE Trans. Pattern Anal. Mach. Intell.*, vol. PAMI-8, no. 6, pp. 679–698, Nov. 1986.
- [8] M. Sharifi, M. Fathy, and M. T. Mahmoudi, "A classified and comparative study of edge detection algorithms," in *Proc. Int. Conf. Inf. Technol. Coding Comput.*, Apr. 2002, pp. 117–120.
- [9] M. C. Shin, D. Goldgof, and K. W. Bowyer, "An objective comparison methodology of edge detection algorithms using a structure from motion task," in *Proc. Conf. IEEE Comput. Vis. Pattern Recognit.*, Jun. 1998, pp. 190–195.
- [10] L. Breiman, J. Friedman, C. J. Stone, and R. A. Olshen, *Classification and Regression Trees*. Boca Raton, FL, USA: CRC Press, 1984.
- [11] K. Kapach, E. Barnea, R. Mairon, Y. Edan, and O. Ben-Shahar, "Computer vision for fruit harvesting robots—State of the art and challenges ahead," *Int. J. Comput. Vis. Robot.*, vol. 3, nos. 1–2, pp. 4–34, 2012.
- [12] R. Berenstein, "A human-robot cooperative vineyard selective sprayer," Ph.D. dissertation, Dept. Ind. Eng. Manage., Ben-Gurion Univ. Negev, Beersheba, Israel, 2016.
- [13] R. Berenstein and Y. Edan, "Robotic precision spraying methods," presented at the ASABE Annu. Int. Meeting, Dallas, TX, USA, 2012, paper no: 121341054.
- [14] R. Berenstein and Y. Edan, "Evaluation of marking techniques for a human-robot selective vineyard sprayer," in *Proc. Int. Conf. Agricult. Eng. (CIGR-AgEng)*, Valencia, Spain, 2012, p. C-1090.
- [15] R. Berenstein and Y. Edan, "Human-robot cooperative precision spraying: Collaboration levels and optimization function," in *Proc. Symp. Robot Control (SYROCO)*, Dubrovnik, Croatia, 2012, pp. 799–804.
- [16] R. Berenstein, Y. Edan, and I. Ben Halevi, "A remote interface for a human-robot cooperative vineyard sprayer," in *Proc. Int. Soc. Precision Agricult. (ICPA)*, Indianapolis, IN, USA, 2012, pp. 15–18.
- [17] R. Berenstein, O. B. Shahar, A. Shapiro, and Y. Edan, "Grape clusters and foliage detection algorithms for autonomous selective vineyard sprayer," *Intell. Service Robot.*, vol. 3, no. 4, pp. 233–243, 2010.
- [18] R. Berenstein, "A human-robot cooperative vineyard selective sprayer," Ph.D. dissertation, Dept. Ind. Eng. Manage., Ben-Gurion Univ. Negev, Beersheba, Israel, 2016.
- [19] R. Berenstein, M. Hočevár, T. Godeša, Y. Edan, and O. Ben-Shahar, "Distance-dependent multimodal image registration for agriculture tasks," *Sensors*, vol. 15, no. 8, pp. 20845–20862, 2015.
- [20] M. A. S. Arikan and T. Balkan, "Process modeling, simulation, and paint thickness measurement for robotic spray painting," *J. Robot. Syst.*, vol. 17, no. 9, pp. 479–494, 2000.
- [21] D. C. Conner, A. Greenfield, P. N. Atkar, A. A. Rizzi, and H. Choset, "Paint deposition modeling for trajectory planning on automotive surfaces," *IEEE Trans. Autom. Sci. Eng.*, vol. 2, no. 4, pp. 381–392, Oct. 2005.
- [22] X. D. Diao, S. X. Zeng, and V. W. Y. Tam, "Development of an optimal trajectory model for spray painting on a free surface," *Comput. Ind. Eng.*, vol. 57, no. 1, pp. 209–216, 2009.
- [23] P. J. From, J. Gunnar, and J. T. Gravidahl, "Optimal paint gun orientation in spray paint applications—Experimental results," *IEEE Trans. Autom. Sci. Eng.*, vol. 8, no. 2, pp. 438–442, Apr. 2011.
- [24] C. Wei and Z. Dean, "Tool trajectory optimization of robotic spray painting," in *Proc. Int. Conf. Intell. Comput. Technol. Autom.*, Oct. 2009, pp. 419–422.
- [25] A. Zaki and M. Eskander, "Spray painting of a general three-dimensional surface," in *Proc. IEEE Int. Conf. Intell. Robot. Syst. (IROS)*, Nov. 2000, pp. 2172–2177.
- [26] G. Pergher and R. Petris, "Pesticide dose adjustment in vineyard spraying and potential for dose reduction," *Agricult. Eng. Int., CIGR J.*, no. 8, pp. 011–020, 2008.
- [27] S. Singh, T. F. Burks, and W. S. Lee, "Autonomous robotic vehicle development for greenhouse spraying," *Trans. Amer. Soc. Agricult. Eng.*, vol. 48, no. 6, pp. 2355–2361, 2005.
- [28] D. C. Slaughter, D. K. Giles, and D. Downey, "Autonomous robotic weed control systems: A review," *Comput. Electron. Agricult.*, vol. 61, no. 1, pp. 63–78, 2008.
- [29] B. L. Steward, L. F. Tian, and L. Tang, "Distance-based control system for machine vision-based selective spraying," *Trans. Amer. Soc. Agricult. Eng.*, vol. 45, no. 5, p. 1255, 2002.
- [30] A. Mandow, J. M. Gomez-de-Gabriel, J. L. Martinez, V. F. Munoz, A. Ollero, and A. Garcia-Cerezo, "The autonomous mobile robot AURORA for greenhouse operation," *IEEE Robot. Autom. Mag.*, vol. 3, no. 4, pp. 18–28, Dec. 1996.
- [31] D. J. Zhao, Y. Zhao, X. L. Wang, and B. Zhang, "Theoretical design and first test in laboratory of a composite visual servo-based target spray robotic system," *J. Robot.*, vol. 2016, pp. 1–11, Mar. 2016.
- [32] J. A. Gázquez, N. N. Castellano, and F. Manzano-Agugliaro, "Intelligent low cost telecontrol system for agricultural vehicles in harmful environments," *J. Cleaner Prod.*, vol. 113, pp. 204–215, Feb. 2016.
- [33] Y. Guan, D. Chen, K. He, Y. Liu, and L. Li, "Review on research and application of variable rate spray in agriculture," in *Proc. IEEE 10th Conf. Ind. Electron. Appl. (ICIEA)*, Jun. 2015, pp. 1575–1580.

- [34] T. W. Berge, S. Goldberg, K. Kaspersen, and J. Netland, "Towards machine vision based site-specific weed management in cereals," *Comput. Electron. Agricult.*, vol. 81, pp. 79–86, Feb. 2012.
- [35] G. G. Peteinatos, M. Weis, D. Andújar, V. R. Ayala, and R. Gerhards, "Potential use of ground-based sensor technologies for weed detection," *Pest Manage. Sci.*, vol. 70, no. 2, pp. 190–199, 2014.
- [36] M. Weyrich, W. Yongheng, and M. Scharf, "Quality assessment of row crop plants by using a machine vision system," in *Proc. IECON 39th Annu. Conf. IEEE Ind. Electron. Soc.*, Nov. 2013, pp. 2466–2471.
- [37] Q. Meng, R. Qiu, J. He, M. Zhang, X. Ma, and G. Liu, "Development of agricultural implement system based on machine vision and fuzzy control," *Comput. Electron. Agricult.*, vol. 112, pp. 128–138, Mar. 2015.
- [38] M. Laursen *et al.*, "Dicotyledon weed quantification algorithm for selective herbicide application in maize crops," *Sensors*, vol. 16, no. 11, p. 1848, 2016.
- [39] R. Oberti *et al.*, "Selective spraying of grapevines for disease control using a modular agricultural robot," *Biosyst. Eng.*, vol. 146, pp. 203–215, Jun. 2016.
- [40] M. Pérez-Ruiz *et al.*, "Highlights and preliminary results for autonomous crop protection," *Comput. Electron. Agricult.*, vol. 110, pp. 150–161, Jan. 2015.
- [41] B. Pettersson, K. Schneider, B. Zebhauser, and K. Siercks, "Surface spattering device," U.S. Patent 13 823 539, Mar. 20, 2014.
- [42] F. Rovira-Más, C. Millot, and V. Sáiz-Rubio, "Navigation strategies for a vineyard robot," presented at the ASABE Annu. Int. Meeting, New Orleans, LA, USA, paper no: 152189750, 2015.



Ron Berenstein received the B.Sc. degree in mechanical engineering and the M.Sc. and Ph.D. degrees in industrial engineering from the Ben-Gurion University of the Negev, Beersheba, Israel, in 2006, 2010, and 2016 respectively.

Since 2007, he has been a Research Engineer with the Agricultural Research Organization-Volcani Center, Rishon LeZion, Israel. Since 2011, he has contributed to the advanced R&D at Ben-Gurion University, on the development of a human robot cooperative vineyard sprayer.



Yael Edan (M'88) received the B.Sc. degree in computer engineering and the M.Sc. degree in agricultural engineering from the Technion-Israel Institute of Technology, Haifa, Israel, in 1984 and 1988, respectively, and the Ph.D. degree in engineering from Purdue University, West Lafayette, IN, USA, in 1990.

She is currently a Full Professor of Industrial Engineering with the Ben-Gurion University of the Negev, Beersheba, Israel, and the current Director of the Agricultural, Biological, and Cognitive Robotics Initiative. She has performed research in robotics, sensors, simulation, and decision-making systems. In addition, she has made major contributions to the introduction and application of intelligent automation and robotic systems to the field of agriculture with several patents.